Volume 16, Issue 2, 162514 (1-14)

International Journal of Nano Dimension (IJND)

https://doi.org/10.57647/j.ijnd.2025.1602.14

Utilize polypropylene-titanium dioxide nano-composite, graphene oxide-chitosan-bentonite nano-absorbent, and straw to remove petroleum hydrocarbons in aquatic environments aggressively

Shahram Azad Zarabadi, Aptin Rahnavard*, Farid Gholamreza Fahimi, Keyvan Saeb

Department of Environment, Tonekabon Branch, Islamic Azad University, Tonekabon, Iran.

***Corresponding author:** rahnavard_aptin@yahoo.com

Original Research

Received:
29 September 2024
Revised:
27 November 2024
Accepted:
4 December 2024
Published online:
1 April 2025

Abstract:

Mitigating petroleum pollutants from wastewater is a critical concern in environmental engineering. Various methods are employed for the removal of these pollutants from wastewater. This research focused on developing adsorbents for the absorption of PAHs from nanocomposites and natural and synthetic materials. Polypropylene fiber-titanium dioxide (PPTO) nanocomposite, graphene oxide-chitosan-bentonite (GOCB) Nano-absorbent, Straw (ST), and a combination of these adsorbents (CB) Nano-absorbents were employed to remove oil pollutants. The experiments were conducted under different acidity levels, varying concentrations of effluent and absorbent, and other retention times. FTIR, SEM, XRD, and GC tests were performed to determine the absorption rate. The results demonstrated that the PPRO nanocomposite and the combination of adsorbents and exhibited the highest removal efficiency, achieving a remarkable 97% removal of petroleum hydrocarbons at a concentration of 10 mg/L. Among the other groups, Straw demonstrated a high absorption rate of 93%, while GOCB showed the lowest rate of 80%. Furthermore, the study identified pH 10 as optimal for PPTO and ST, whereas GOCB performed best at pH 3. Augmenting the adsorbent dosage improved pollutant removal; however, surpassing the optimal level did not result in further enhancements. These findings highlight the potential of the PPTO nanocomposite as a promising solution for eliminating petroleum hydrocarbons from oil-contaminated water, thus contributing to developing effective strategies for addressing oil pollution in aquatic environments.

Keywords: Absorbent; Graphene oxide-chitosan-bentonite (GOCB); Nanoparticles; Petroleum hydrocarbon; Wastewater

1. Introduction

Industrial activities have caused environmental damage by accumulating harmful substances like oil hydrocarbons in water and soil ecosystems [1]. Petroleum is toxic to the environment and a significant pollutant due to its ability to dissolve cell membranes and disrupt plant root structures [2]. Pollution is caused by the direct entry of pollutants into the ecosystem, as well as their natural release from reservoirs, extraction, transfer, refining, and consumption activities. This pollution can be absorbed by soil or organic particles, gradually increasing their concentration as they flow towards water bodies [3].

Petroleum compounds can seep into the ground, contaminating the food chain and posing a risk to plants, animals, and humans [4]. Petroleum compounds can seep into the ground, contaminating the food chain and posing a risk to plants, animals, and humans [5]. When leaked, petroleum compounds can move through the soil via capillary and gravity forces, filling the soil pores. In the case of significant leakage, the liquid phase can reach the water surface and travel with the underground water flow, floating due to its lower density than water [6]. This type of pollution can impact people through various pathways, including breathing polluted air, skin absorption, use of petroleum-based products, consumption of contaminated water or plants, and consumption of animals that have ingested contaminated plants [7]. Methods for purifying water contaminated

with petroleum compounds include absorption, filtration, membrane processes, coagulation, advanced oxidation, and stabilization ponds [8, 9].

Oil spills are currently removed from water and paved roads using mechanical, biological, chemical, and absorption techniques [10, 11]. Nanoscience offers a sustainable solution to enhance post-oil spill response technology. Nanomaterials, especially nanocomposites, provide superior performance compared to pure matrix materials [12, 13]. Nanoscience is a sustainable and efficient solution for improving post-oil spill response technology. Nanomaterials, particularly nanocomposites, play a crucial role in this process by offering superior performance compared to pure matrix materials [14]. The use of nanomaterials and nanocomposites in surface adsorption presents a promising approach for the more efficient and effective removal of oil pollutants, contributing to environmental preservation and remediation efforts [15]. Nanoscience is potentially a sustainable solution to enhance post-oil spill response technology, where at nanoscale; materials can be functionalized for very specific purposes, such as the formation of emulsions or magnetic adsorbents. The use of nanotechnology for water treatment has been studied for about 20 years, but its use for oil spill recovery is a newer field that has grown almost exponentially in the past 10 years. The ability to absorb a set of absorbent nanoparticles of petroleum hydrocarbons is compared separately at the beginning, and at the end, a combination of all of them is considered as a Nano absorbent complex [16]. In this way, the efficiency of these materials will be well determined.

The PP-TiO_2 nanocomposite combines titanium dioxide nanoparticles with a polypropylene matrix to create a material with exceptional oil-absorbing and water-repellent properties. The polypropylene matrix is simple in structure, highly flexible, lightweight and water-repellent [17]. The mechanical properties remain unchanged even when in contact with water, ensuring its reliability as an absorbent [18]. Adding titanium dioxide nanoparticles to polypropylene improves the nanocomposite's ability to absorb oil from water [19].

"Graphene oxide is important for removing pollutants as a nanostructure" [20]. Graphene-based nanoparticles have high adsorption capacity and large specific surface area, making them effective in addressing water pollution. Graphene oxide, derived from graphene, has significant surface area and strong mechanical properties [21]. Graphene oxide's hydrophilic nature allows it to disperse easily in solvents while remaining stable. Its capacity for large-scale production makes it practical for industrial applications [22].

Biopolymers like chitin and chitosan are increasingly used for absorbing pollutants [23]. These biopolymers are safe, easily accessible, and inexpensive, allowing them to efficiently absorb and eliminate pollutants, even at low levels [24]. Chitosan and graphene oxide nanoparticles have properties that make them effective at adsorbing pollutants. Chitosan can interact with aromatic compounds, while graphene oxide nanoparticles have high adsorption capacity and specific surface area [25]. When combined with modified bentonite, it effectively removes oil contaminants from water and improves the adsorption of petroleum compounds [26].

Moreover, researchers are actively investigating cost-effective and readily available adsorbents derived from agriculture and biology [27]. Straw holds promise due to its abundance of lignocellulosic fibers, proteins, carboxyl, hydroxyl, and amino groups [28]. Straw is an ideal option for adsorption processes because of its abundance and diverse functional groups that enhance its effectiveness in adsorbing various substances [29]. This study aims to evaluate the adsorption capabilities of three specific absorbents-PPTO, GOCB, and ST-for removing hydrocarbon-based petroleum compounds from water. Initially, each absorbent will be individually assessed to determine its adsorption capacity for hydrocarbon pollutants [30]. The study examines how well a combination of these absorbents (CB group) can remove hydrocarbon pollutants from water [31–33].

2. Materials and methods

2.1 Preparing samples

The devices, sampling method and tests that have been used are: Model ultrasonic device TAT (Homogenize the solution), X-ray diffraction (XRD) model Philips-pw1730 (Available crystal phases, crystal size), Electron microscope (SEM) along with XRF model FEI-Nova: SEM (Shapes and sizes of particles, particle composition), Infrared spectroscopy (FTIR) model Brucker (Types of chemical bonds available), Visible-ultraviolet spectroscopy (UV-Vis) model Perklin (absorption rate), Gas chromatography (GC-FID) model Agilent6890, (Identification of organic compounds) Oven model shimaz. (To dehumidify the sample) list of materials used in the research. We Used TiO_2 manufacturing company Merc, Polypropylene Nano fibers manufacturing company NSG, $C_{140}H_{42}O_{20}$ manufacturing company Merc, C_xH_y manufacturing company Merc, $C_6H_{11}NO_4$ manufacturing company Merc, $H_2Al_2O_6Si$ manufacturing company Merc, H_2SO_4 manufacturing company Merc, NaOH manufacturing company Merc.

Samples were taken from the surface sewage of District 18 in Tehran at the outlets leading to the Azadegan Highway during two seasons: low precipitation (summer 2022) and high rainfall (autumn 2021). The samples were tested for petroleum pollutants, showing contamination with hydrocarbon compounds only during the high precipitation season. In the lab, we prepared wastewater using a solution of 16 multi-ring aromatic hydrocarbons from Sigma Aldrich to assess the adsorption capacity of each absorbent. We used a standard solution with a concentration of 500 milligrams per liter for each aromatic hydrocarbon, and lower standards in the aqueous solution to mimic wastewater containing PAHs (Polycyclic Aromatic Hydrocarbons).

2.2 Preparing absorbents

2.2.1 Nanocomposite of polypropylene and titanium dioxide nanoparticles

The study involved mixing 1-centimeter-long polypropylene fibers with a diameter of 330 micrometers with titanium dioxide nanoparticles, which were produced by the Iranian Nanomaterials Pioneers Company. The nanoparticles con-

sisted of 80% anatase and 20% rutile, with a 20-nanometer diameter. The fibers were heated to 64 degrees Celsius for 90 minutes in the presence of activated moisture to maximize absorption efficiency while preserving their natural structure [34]. An aqueous dispersion of TiO_2 nanoparticles was prepared at concentrations of 0.5, 1, and 2 grams per liter. Then, 5 grams of fibers were combined with 1 gram of titanium dioxide nanoparticles in 500 milliliters of distilled water. To prevent nanoparticle aggregates during the mixing process, the modification of the polypropylene nanofibers with the TiO_2 water dispersion was carried out using ultrasound at 40 °C for 30 minutes, with a power of 100 watts and a frequency of 26 kilohertz [35]. The nanocomposite was dried at 40 °C, washed with distilled water, and then dried at 35 °C for 48 hours.

2.3 Graphene oxide-chitosan-bentonite

To prepare the solution, 0.1 grams per liter of chitosan (obtained from Sigma) was added to 50 milliliters of distilled water and mixed with acetic acid in a 24:2 ratio (water to acetic acid). The mixture was homogenized for 30 minutes. Meanwhile, in a separate container, 0.2 grams per liter of graphene oxide nanoparticles (manufactured by Agricultural, India) and 0.2 grams per liter of bentonite (manufactured by Merck) were combined in 50 milliliters of distilled water and subjected to ultrasonication for 30 minutes to ensure homogeneity. Subsequently, the two solutions were combined and refluxed for 3 hours at a temperature of 60 degrees Celsius. Following refluxing, 1 N sodium hydroxide solution was gradually added to the mixture until it reached a gel-like consistency. The final product went through filtering, washing with water, and drying in an oven at 60 degrees Celsius for 8 hours. The resulting product featured a particle size smaller than 2 millimeters [36].

2.4 Preparing straw

The samples are washed with distilled water, dried at 105 degrees Celsius for 14 hours, shredded using a grinder machine, and sieved to achieve particle sizes smaller than 2 millimeters [37, 38].

2.5 Preparing multi-walled carbon nanotubes (MWCNTs)

I purchased multi-walled carbon nanotubes from Pishgaman Nano Materials Company. The nanotubes have a specific surface area of 233 g/m^2, an inner diameter of $3-5$ nm, an outer diameter of $5-15$ nm, and a length of 50 micrometers, with a purity of more than 95%. I need to analyze the position of functional groups on the nanotubes' surface using scanning electron microscopy (SEM) and determine their size and structure using transmission electron microscopy (TEM). Additionally, I will evaluate the special surface of the nanotubes using Brunauer's BET method and the Emmett & Teller method.

2.6 Preparing absorbents mixture

Mix 0.2 grams of each absorbent with 50 milliliters of distilled water. Agitate the mixture for 20 minutes using an ultrasonic device at 25 degrees Celsius, and then dry it in an oven at 35 degrees Celsius.

2.7 Assessing the efficiency of absorbents in removing petroleum hydrocarbons

2.7.1 Optimal absorption time and concentration of the adsorbents

To determine the most effective absorption time for the absorbents, we introduced 0.01 grams of the absorbent material to 50 milliliters of wastewater with a PAH concentration of 10 milligrams per liter. The mixture was then placed on a shaker at a speed of 140 revolutions per minute. At various time intervals of 10, 60, 120, and 180 minutes, the absorbent was separated from the solution using a centrifuge. The absorption of the solution was then measured using a spectrophotometer to identify the optimal concentration of the Nano-adsorbent. Different quantities of Nano-adsorbent (0.001, 0.01, 0.025, and 0.05 grams) were utilized in 50 milliliters of wastewater with a PAH concentration of 10 milligrams per liter. Once the optimal time had elapsed, the absorbents were separated from the solution, and the absorption was measured using a spectrophotometer to determine the optimal concentration of the Nano-adsorbent.

2.7.2 The effect of pH of the petroleum wastewater on the efficiency of the absorbents

We will analyze the effect of pH on petroleum wastewater by making solutions of PAHs with a concentration of 10 mg/L at pH levels 3, 5, 7, and, 10. Then, we will add the optimal Nano-adsorbent concentration to each solution. After a set time, we will measure the absorption of the solutions using a spectrophotometer [39].

2.7.3 Evaluation of the absorption capacity under optimal conditions

We optimized the conditions and then separated the components. We analyzed the wastewater using gas chromatography to determine the hydrocarbon levels. Hexane was used for extraction. We also conducted FTIR, SEM, and XRD tests to examine the Nano-adsorbent structure before and after absorption [40].

2.8 Investigation of adsorption isotherms, kinetics, and thermodynamics

The adsorption isotherm formula represents the equilibrium amount of the adsorbate material on the adsorbent concerning concentration changes at a constant temperature. The surface adsorption process reaches dynamic equilibrium. Equilibrium data for the adsorption of petroleum pollutants on the Nano-adsorbent were modeled using non-linear equations such as Langmuir, Freundlich, Dubinin-Radushkevich, and Temkin at a temperature of 298 Kelvin. These equations were compared to determine the isotherm the adsorbent follows for each adsorbate [41]. The Langmuir adsorption isotherm is a well-known equation based on the assumption of single-layer adsorption of the adsorbate onto the surface of the adsorbent at a constant temperature [42]. The Langmuir isotherm

equation is given as follows:

$$\log q_e = \frac{q_{\max} K_l C_e}{1 + K_l C_e} \tag{1}$$

The isotherm model explains how a solute is adsorbed onto

a solid surface. In this model, q_e represents the amount of adsorbate adsorbed at equilibrium, $q_{\max}$ is the maximum adsorption capacity of the adsorbent, C_e is the equilibrium concentration of the adsorbate, and K_l is the Langmuir constant. The Freundlich adsorption isotherm is obtained empirically, and its linear form is derived from a specific equation [43].

$$\log q_e = \frac{q_{\max} K_l C_e}{1 + K_l C_e} \tag{2}$$

It is assumed that the adsorption characteristics are related to the porosity of the adsorbent [43]. Which, the Langmuir isotherm equation can describe.

$$\log q_e = \frac{q_{\max} K_l C_e}{1 + K_l C_e} \tag{3}$$

The text covers adsorption parameters and equations including maximum adsorption capacity, the Dubinin-Radushkevich isotherm constant, and the Polanyi potential, calculated using the equation $\varepsilon = RT \ln(1 + 1/C_e)$. The KDR constant determines the average free energy of adsorption. The Temkin adsorption isotherm indicates that the amount of adsorbate is directly related to the logarithm of the adsorbate pressure [42, 43]:

$$\log q_e = \frac{q_{\max} K_l C_e}{1 + K_l C_e} \tag{4}$$

The amount of adsorbate adsorbed at equilibrium is represented by the Temkin isotherm equation:

$$q = B * \ln(KT * C_e)$$

where, q is the amount of adsorbate adsorbed at equilibrium, B is the Temkin constant, KT is the Temkin adsorption potential (in units of L/g), and C_e is the equilibrium concentration of the adsorbate. Additionally, pseudo-first-order, pseudo-second-order, and intra-particle diffusion models are used to study surface adsorption at a temperature of 298 Kelvin. The thermodynamics of adsorption are investigated in the temperature range of 25 to 75 degrees Celsius using the Van't Hoff equation, and the parameters of entropy, enthalpy, and Gibbs free energy are calculated. The thermodynamic equilibrium constant, K_c, is obtained from the following relationship.

$$K_c = q_e / C \tag{5}$$

Furthermore, the relationship between Gibbs free energy and K_c is determined using the equation:

$$G_0 = RT \ln K_c \tag{6}$$

3. Results and discussions:

3.1 Factors examined in the removal of petroleum hydrocarbons

3.1.1 Time and absorbent concentration

Adsorption increases rapidly in the first few minutes, with over 50% occurring within the initial ten minutes. After 180 minutes, the adsorption rate gradually decreases and reaches a plateau. No significant difference in the adsorption percentage was observed between minutes 120 and 180. Compared to other groups, the polypropylene-titanium dioxide nanocomposite exhibited higher initial adsorption, and the decrease in adsorption rate occurred abruptly. All groups, except for the Graphene Oxide-Chitosan-Bentonite Nano-adsorbent, reached their maximum adsorption level after 120 minutes, and their adsorption curves remained constant thereafter. However, the adsorption of graphene oxide-chitosan-bentonite-Nano-adsorbent continued until 180 minutes (Fig. 1).

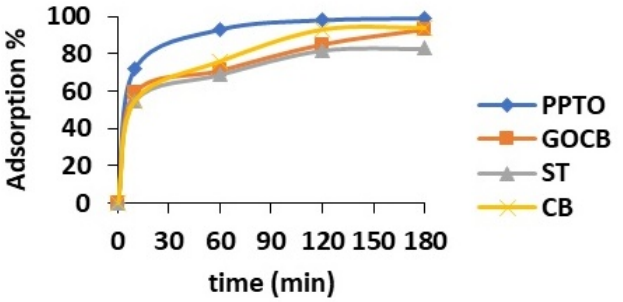

Figure 1. Adsorption Capacity of Adsorbents (Polypropylene-Titanium Dioxide Nano-composite (PPTO), Graphene Oxide-Chitosan-Bentonite Nano-absorbent (GOCB), Straw (ST), Combination (CB)) over Time: The PPTO shows higher initial adsorption, while the GOCB continues adsorption until 180 minutes. Other groups reach maximum adsorption after 120 minutes, maintaining constant curves thereafter.

Based on the data presented in figure 2, it was observed that higher adsorption capacity for the pollutant is achieved with an increase in adsorbent dosage. However, it was noted that beyond a certain concentration level for each group, there was no significant improvement in adsorption capacity, with the exception of polypropylene-titanium dioxide nanocomposite, which exhibited almost complete absorption of the pollutant as its concentration reached 1 mg/L.

3.1.2 Impact of the petroleum wastewater pH

The water efficiency in alkaline pH conditions is generally consistent, except for the GOCB Nano adsorbent. On the other hand, the adsorption capacity of the PPTO fluctuates from acidic to neutral pH but significantly increases in alkaline pH conditions. In contrast, the adsorption capacity

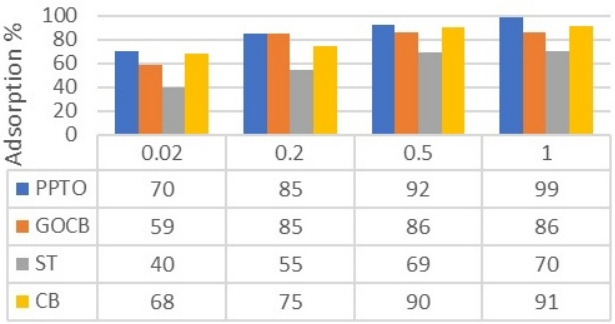

	0.02	0.2	0.5	1
PPTO	70	85	92	99
GOCB	59	85	86	86
ST	40	55	69	70
CB	68	75	90	91

Figure 2. Impact of Adsorbent Concentration on Adsorption Capacity: Increasing the adsorbent dosage enhances pollutant adsorption, except for concentrations beyond a certain level. The polypropylene-titanium dioxide nanocomposite shows remarkable adsorption, nearly eliminating the pollutant up to 1 mg/L.

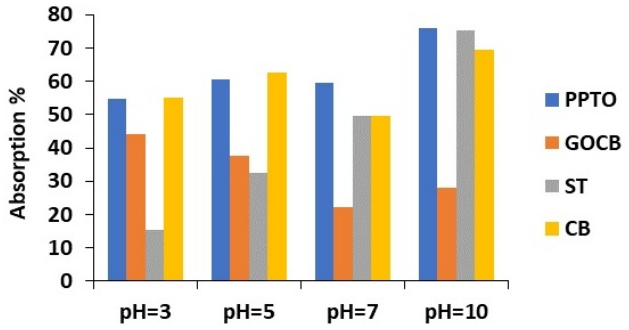

Figure 3. Effect of pH on Adsorption Capacity: Alkaline pH conditions generally enhance adsorption efficiency, except for the GOCB Nano adsorbent. GOCB's capacity decreases with decreasing acidity but slightly increases at pH = 10.

of the GOCB Nano adsorbent decreases as the acidity decreases, but it shows a slight increase at pH 10 (Fig. 3). In order to check the performance of the synthesized nanocomposites, its zeta potential was determined (Fig. 4). The zeta potential test measures the electric potential difference between the sliding layer and the potential at a distance from the particle (a distance with zero potential) and has a direct relationship with the surface charge density of the particles. Zeta potential analysis is a method to determine the electric charge of particles, the high charge of particles, both negative and positive, leads to the stability of particles in liquids and their non-clumping and sedimentation. On the other hand, the charge of particles is effective in how they interact with other molecules.

3.1.3 Adsorption capacity under optimal conditions

The specific adsorption capacity for each adsorbent can be found in Table 1.

Under optimal conditions (including incubation time, adsorbent concentration, and pH), the wastewater samples underwent GC analysis (Fig. 5).Resents the results of PAH extraction from the samples following adsorption under the determined optimal conditions. The Table 2, provides the corresponding concentration values in parts per million (ppm).

Based on the data obtained (figure 6), the use of PPTO nanocomposite has resulted in a more effective removal of naphthalene.

3.1.4 Characterization of the adsorbents pre and post-absorption

The spectrum of the polypropylene and titanium dioxide nanocomposite fibers, before and after use for pollutant adsorption, reveals absorption peaks at 456.3, 1544.25, 2897, 1717, 1618, and 1048 cm^{-1}. These peaks correspond to the stretching vibrations of Ti-O, Ti-OH, C-H, C=O, C=C, and C-O, respectively. The fact that these peaks are still present after the use of the Nano-adsorbents indicates the

Table 1. (PPTO), Graphene Oxide-Chitosan-Bentonit Nano-absorbent (GOCB), Straw (ST), Combination (CB)).

Absorbent	Optimal pH	Optimal Absorbent Concentration (mg/L)	Optimal Contact Time (min)
PPTO	10	1	120
GOCB	3	0.2	180
ST	10	0.5	120
CB	10	0.5	120

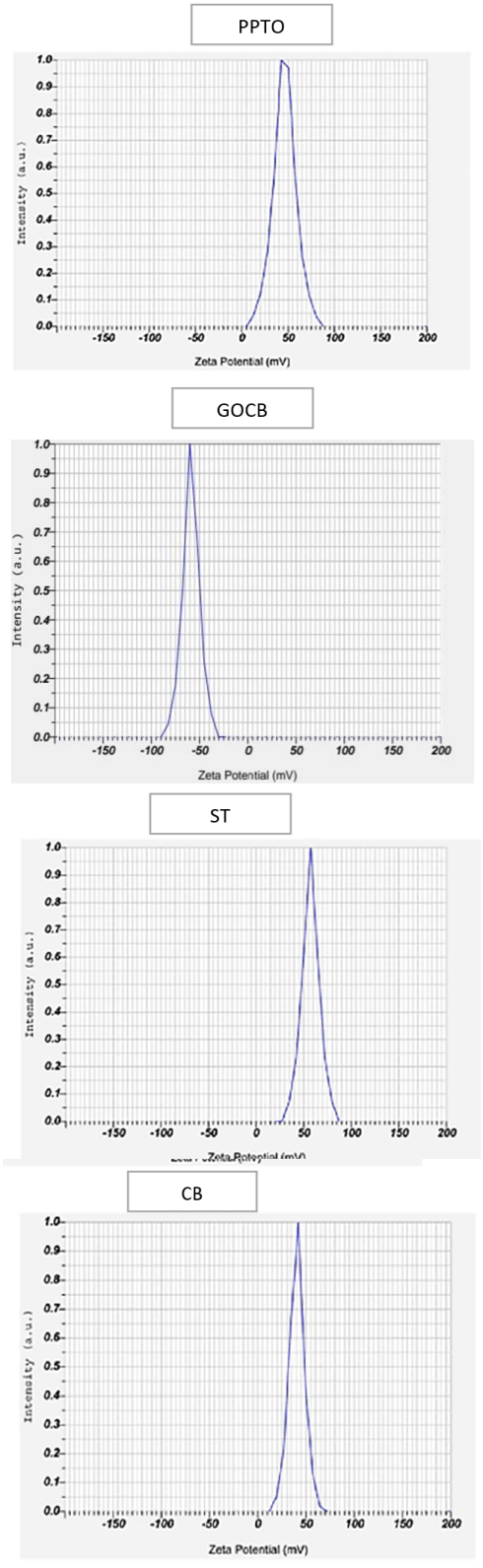

Figure 4. ZETA potential of Adsorbents (Polypropylene-Titanium Dioxide Nano-composite (PPTO), Graphene Oxide-Chitosan-Bentonite Nano-absorbent (GOCB), Straw (ST), Combination (CB)) over intensity.

Table 2. (PPTO), Graphene Oxide-Chitosan-Bentonit Nano-absorbent (GOCB), Straw (ST), Combination (CB).

	Naphthalene	Acenaphthene	2-Bromonaphthalene	Acenaphthylene	Flourene	Anthracene	Phenanthrene	Flouranthene	Pyrene	Benzo (A) Anthracene	Chrysene	Benzo (B) Fluoranthene	Benzo (A) Pyrene	Indeno (1,2,3-CD)	Benzo (G,H,I) Perylene	total PAHs (ppm)
Control	0.7	0.7	0.7	0.7	0.7	0.7	0.7	0.7	0.7	0.7	0.7	0.7	0.7	0.7	0.7	10.5
PPTO	0	0	0	0	0.13	0	0	0	0	0	0	0	0	0	0	0.13
GOCB	0.352	0.534	0	0.352	0.304	0.122	0	0	0	0	0.346	0	0	0	0	2.01
ST	0.13	0.188	0	0	0.216	0	0	0	0	0	0.18	0	0	0	0	0.714
CB	0	0	0	0.192	0.16	0	0	0	0	0	0	0	0	0	0	0.352

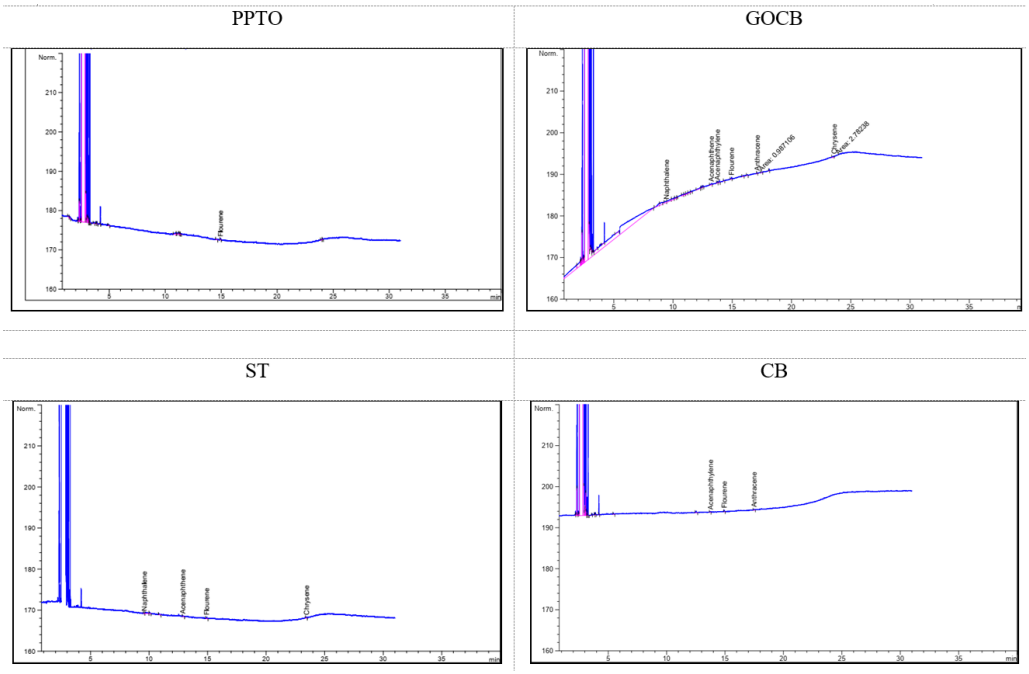

Figure 5. Chromatogram of Petroleum Wastewater after Adsorption by Adsorbents.

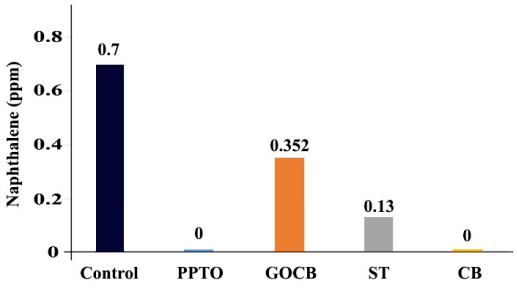

Figure 6. Comparison of Naphthalene Removal by Different Adsorbents: data demonstrates the superior performance of PPTO and CB (combination of adsorbents) groups in reducing naphthalene levels. The straw adsorbent achieves a significant one-fifth reduction, while GOCB reduces levels by half.

desirable recoverability and high stability of the synthesized nanocomposite. It's worth noting that other adsorbents also retain their absorption peaks in the FTIR spectrum after being used for pollutant adsorption.

Based on the results obtained from the X-ray diffraction (XRD) analysis of the adsorbents (see figure. 7), it is evident that all the diffraction peaks present in the XRD pattern of the adsorbents remain unchanged even after being used as pollutant adsorbents. This indicates that the adsorbents remain intact after use. However, slight variations may suggest minor changes in the crystalline structure of the adsorbents used.

To analyze the morphology, particle shape, porosity, and particle size distribution, scanning electron microscopy (SEM) was used. Figure 8 displays the SEM images of the Nano-adsorbents, revealing the presence of defects and voids. These imperfections diminish when hydrocarbons are adsorbed on the adsorbent surface, suggesting a high adsorption capacity for petroleum hydrocarbons (Fig. 9).

3.1.5 Adsorption Isotherms, Kinetics, and Thermodynamics

Adsorbents were analyzed using four models: Langmuir, Freundlich, Dubinin-Radushkevich, and Temkin. Corre-

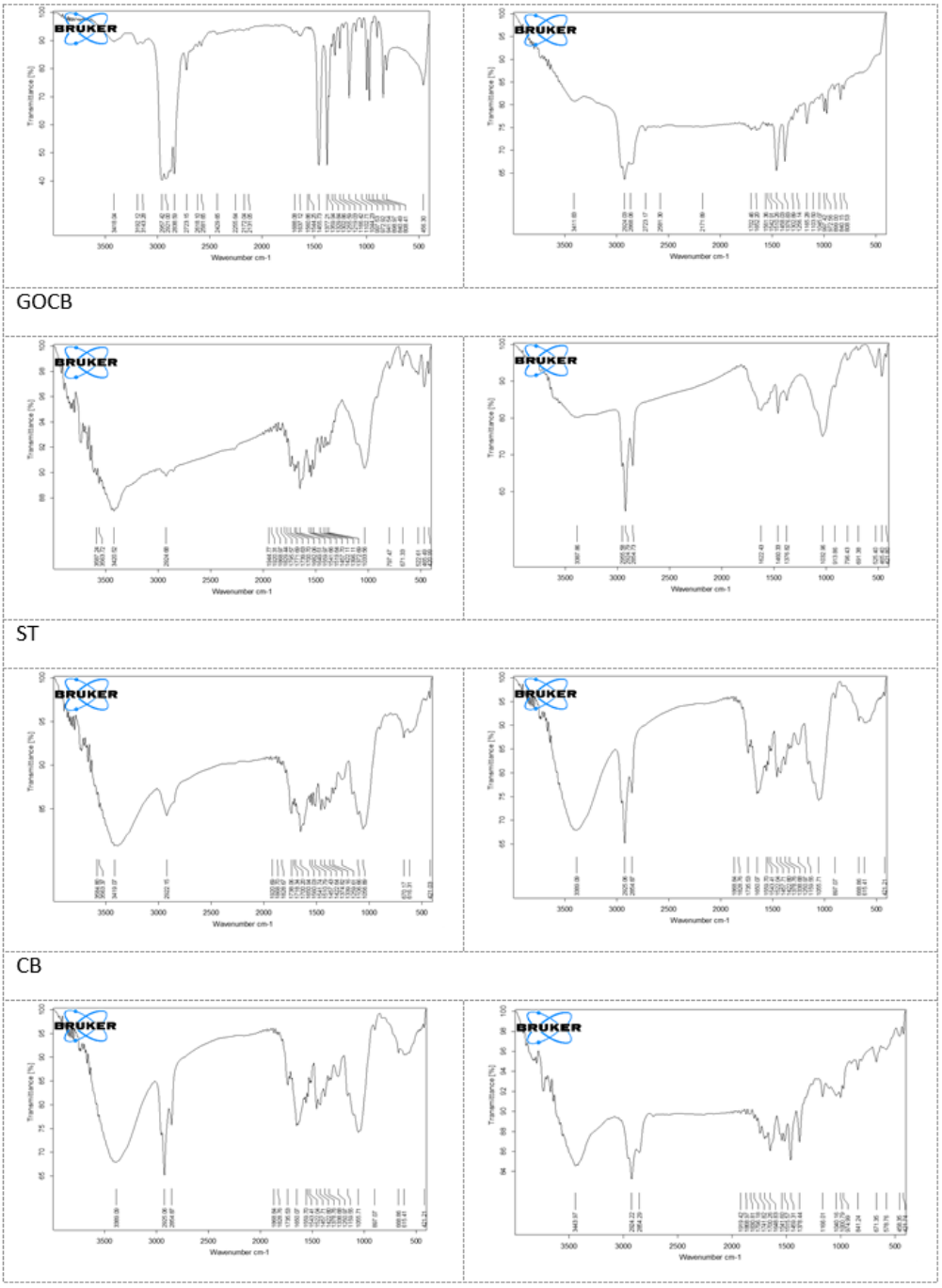

Figure 7. FTIR Analysis of adsorbents: The FTIR spectrum reveals absorption peaks corresponding to different vibrations before and after pollutant adsorption. The preserved peaks indicate the recoverability and stability of the adsorbents.

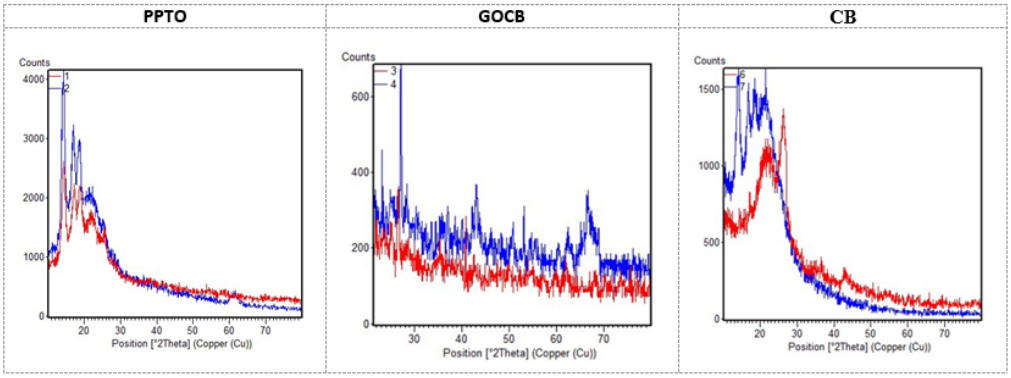

Figure 8. XRD Analysis of Adsorbents: Patterns show preserved diffraction peaks after pollutant adsorption, indicating their integrity. Minor variations suggest slight changes in the crystalline structure.

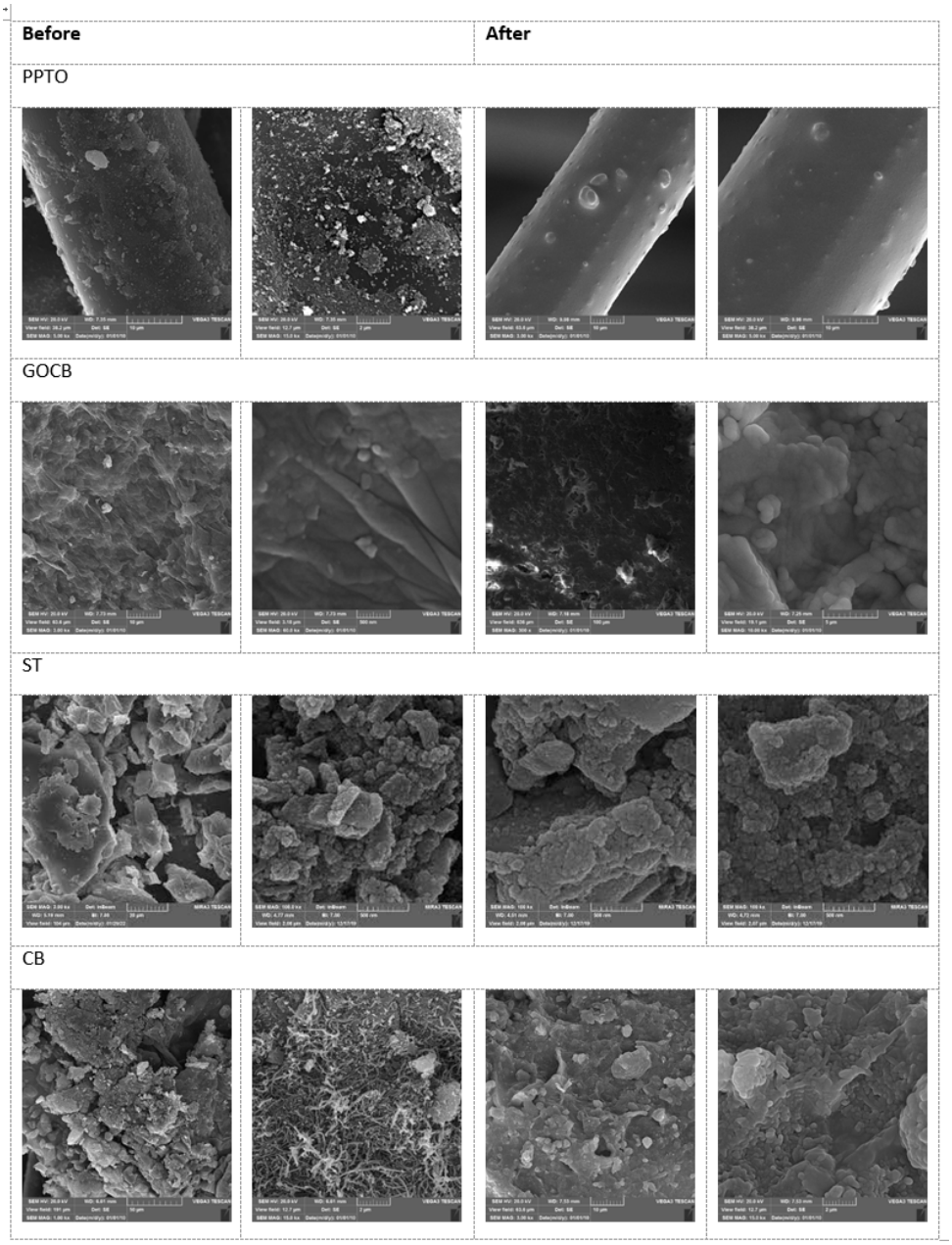

Figure 9. SEM Analysis of Adsorbents: Defects and voids decrease post-hydrocarbon adsorption, indicating the high adsorption capacity for petroleum hydrocarbons.

Table 3. Chemical Composition Analysis of Straw Sample using XRF.

SiO_2 %	Al_2O_3 %	Fe_2O_3 %	CaO %	MgO %	Na_2O %	K_2O %	TiO_2 %	MnO %	P_2O_5 %
0.432	-	0.212	3.863	0.517	0.209	4.284	0.028	0.05	0.519
S (ppm)	Cl (ppm)	Ba (ppm)	Co (ppm)	Cr (ppm)	Cu (ppm)	Mo (ppm)	Ni (ppm)	Sr (ppm)	V (ppm)
4630	5603	-	-	5	8	-	26	140	24
Ce (ppm)	La (ppm)	Pb (ppm)	Zr (ppm)	Zr (ppm)					
28	-	-	-	-					

sponding equations and linear trendlines for the adsorbents are available in Table 4 and figures 9 to 13.

The research delved into the absorption of petroleum hydrocarbons by absorbents through analyzing reaction rate plots for first-order, second-order, and intra-particle diffusion reactions. Table 3 presents the Adsorption Kinetic Parameters derived from the analysis, confirming that the absorption reaction follows a second-order rate equation. Furthermore, the study explored the thermodynamics of surface adsorption of petroleum hydrocarbons at temperatures between 25 and 75 degrees Celsius. The results in Table 4 display the calculated values of ΔG°, ΔH°, ΔS°, and R^2, crucial thermodynamic parameters for the adsorption process. The obtained ΔG° values indicate that the adsorption process is generally spontaneous and exothermic. Notably, raising the temperature from 25 to 75 degrees Celsius enhanced the efficiency of petroleum hydrocarbon removal.

This article discusses a study that evaluates the adsorption potential of various absorbents for removing hydrocarbon-based petroleum compounds from water. The study examines Polypropylene-Titanium Dioxide Nanocomposite (PPTO), Graphene Oxide-Chitosan-Bentonite Nano-absorbent (GOCB), and Straw (ST), as well as the potential of combining them (CB). The study aims to assess their individual adsorption capacities. Titanium Dioxide (TiO_2) and Graphene Oxide are known for their effectiveness in removing pollutants from water. Additionally, straw has shown promise in removing color from water solu-

Table 4. Adsorption Kinetic Parameters for Petroleum Hydrocarbon Removal by absorbents.

	1st order kinetics		**2nd order kinetics**		**Intraparticle diffusion**	
Absorbent	**R^2**	**k(min^{-1})**	**R^2**	**k(min^{-1})**	**R^2**	**k(min^{-1})**
PPTO	0.93	0.045	0.99	0.098	0.87	0.26
GOCB	0.79	0.008	0.98	0.1	0.98	0.33
ST	0.92	0.03	0.99	0.11	0.96	0.29
CB	0.92	0.033	0.99	0.099	0.95	0.4

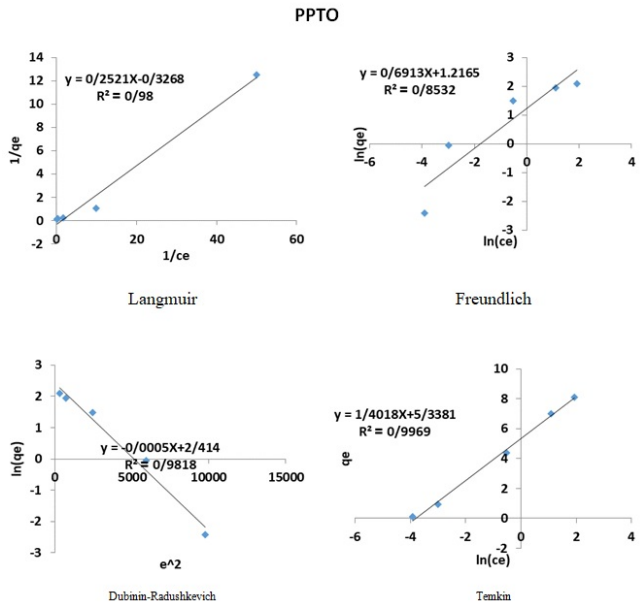

Figure 10. Isotherm Analysis of Polypropylene-Titanium Dioxide Nanocomposite (PPTO) Adsorbent: The Langmuir, Freundlich, Dubinin-Radushkevich, and Temkin models are applied to calculate the adsorption isotherms, and their corresponding linear trendlines are shown.

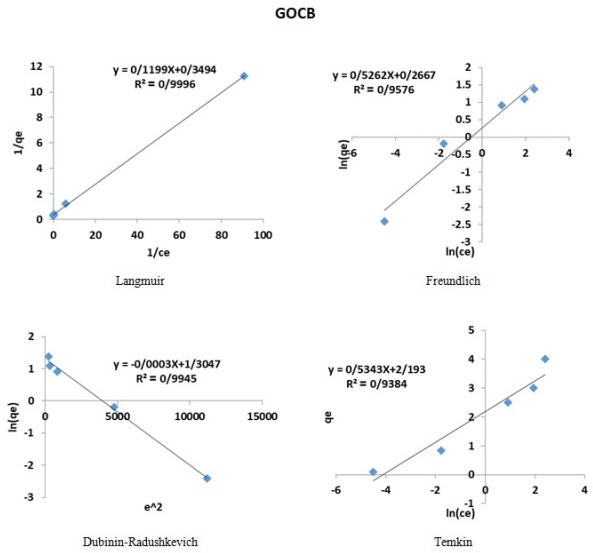

Figure 11. Isotherm Analysis of Graphene Oxide-Chitosan-Bentonite Nonabsorbent (GOCB): The Langmuir, Freundlich, Dubinin-Radushkevich, and Temkin models are used to determine the adsorption isotherms, and the resulting linear trendlines are presented.

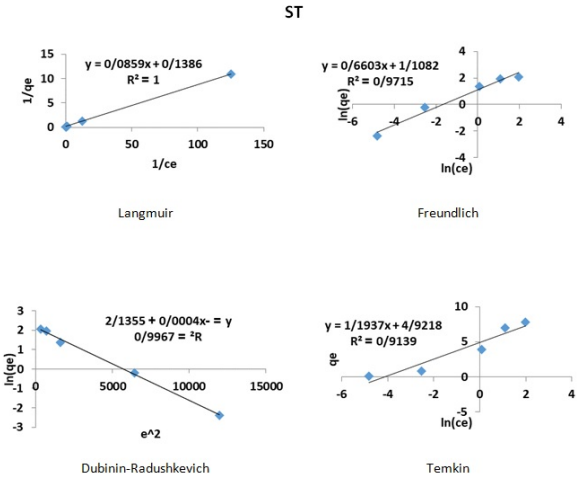

Figure 12. Isotherm Analysis of Straw (ST) Adsorbent: The Langmuir, Freundlich, Dubinin-Radushkevich, and Temkin models are employed to calculate the adsorption isotherms, and their respective linear trendlines are displayed.

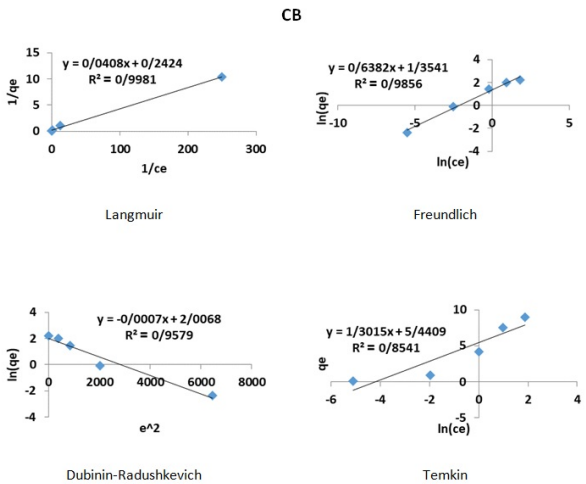

Figure 13. Isotherm Analysis of Combination (CB) Adsorbent: The Langmuir, Freundlich, Dubinin-Radushkevich, and Temkin models are utilized to derive the adsorption isotherms, and the corresponding linear trendlines are depicted.

Table 5. Thermodynamic Parameters of Adsorption Process: The results indicate the spontaneity and exothermic nature of the adsorption process while also highlighting the enhanced efficiency with increasing temperature.

	ΔG° (KJ/mol) at 298 k	ΔH° (KJ/mol)	ΔS° (J/mol.k)	R^2
PPTO	-199	4240	14.896	0.9224
GOCB	-277	3192.2	9.7815	0.9855
ST	-206	2407	8.77	0.9048
CB	-242	2750	10.04	0.9775

tions and industrial effluents [44]. The study found that the polypropylene-titanium dioxide nanocomposite was most effective at pH 10 for removing oil pollutants. However, the graphene oxide-chitosan-bentonite Nano-adsorbent was found to work best at pH 3. Combining all the adsorbents was most effective at pH 10 for removing pollutants increasing the adsorbent dosage leads to a higher adsorption capacity for the targeted pollutant, as confirmed by the study's results and previous research [45]. The adsorption percentage in the polypropylene-titanium dioxide nanocomposite group increases with rising concentrations up to 1 mg/L. The optimal concentration for using the combination of adsorbents and for the straw adsorbent is 0.5 mg/L, while for the graphene oxide-chitosan-bentonite Nano-adsorbent, it is 0.2 mg/L. Exceeding the optimal concentrations does not enhance the adsorption capacity; instead, it can decrease performance. It's generally advisable to use an optimal dosage of Nano-adsorbents to maximize removal efficiency [46]. This decline can be attributed to the aggregation of the adsorbent material, which reduces the availability of active sites for pollutant adsorption [47, 48]. The study did not show a decline, indicating that the concentrations of adsorbents used were likely appropriate. However, the adsorbent materials effectively demonstrated impressive efficacy in adsorbing pollutants. [49].

The study revealed that oil pollutants are more effectively absorbed by adsorbent materials with longer contact time. The adsorption capacity of the polypropylene-titanium dioxide nanocomposite increases steadily up to 120 minutes. Beyond 120 minutes, there is little difference in adsorption, suggesting a constant rate. These findings align with Shah Rezaei's previous study in (2012) [50]. The graphene oxide-chitosan-bentonite Nano-adsorbent takes a longer time for effective adsorption, typically around 160 minutes. Other studies have reported a shorter time of around 45 minutes for the absorption of pollutants using this adsorbent [51]. The isotherm comparison shows that the polypropylene-titanium dioxide nanocomposite follows the Temkin isotherm, while the graphene oxide-chitosan-bentonite, straw, and combined adsorbents follow the Langmuir isotherm (Table 5 and Figs. 9-13). The investigations show that the adsorption process is spontaneous and exothermic. Increasing the temperature from 25 °C to 75 °C resulted in higher removal efficiency of petroleum hydrocarbons. The adsorption reaction rate follows the second-order rate equation. Characterization of the adsorbents before and after adsorption showed a decrease in absorption within the wave numbers $1350 - 1450$ using FTIR (Fig. 7), indicating the adsorption capability of these materials. The SEM images (Fig. 9) provide additional evidence of the effectiveness of the adsorbents [52]. The images illustrate the buildup of pollutants on the used adsorbent materials, particularly the distribution of metal particles on the polypropylene fibers. A comparison of the images before and after the adsorption process shows a smoother surface of the fibers after the absorption of pollutants. Similar results have been found in other studies, highlighting the reliability of these observations [53].

After the adsorption process, SEM images (Fig. 8) of other adsorbents show compact surfaces and morphologies with filled defects, indicating pollutant adsorption. The polypropylene-titanium dioxide nanocomposite achieved the highest petroleum hydrocarbons removal efficiency at a concentration of 10 milligrams per liter, reaching 97%. Other studies have also shown that titanium dioxide nanoparticles alone have good adsorption capabilities in removing oil-based compounds [54]. The two investigated groups were more effective at removing naphthalene compared to the others. Naphthalene is highly toxic and its water concentration should not exceed 0.05 milligrams per liter. Additionally, it is not easily degradable, making its removal challenging [55]. These two materials have shown great performance and cost-effectiveness, making them suitable for effectively reducing naphthalene levels in oil-contaminated water and wastewater.

3.1.6 Disposal studies for reuse of adsorbents

In order to reuse the Nano adsorbents, they were washed three times using acetone and then washed with distilled water and dried at a temperature of 40 degrees, and this process was done after three absorptions for each Nano adsorbent.

After drying, the Nano absorbents were added again to the aqueous solution containing aromatic hydrocarbons under optimal conditions, and the removal rate of aromatic hydrocarbons was determined through absorption (UV) (Figs. 14,15).

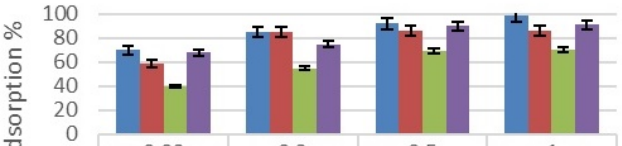

	0.02	0.2	0.5	1
PPTO	70	85	92	99
GOCB	59	85	86	86
ST	40	55	69	70
CB	68	75	90	91

Figure 14. The percentage of error on the graphs.

Table 6. Disposal studies for reuse of adsorbents.

Nano attractant	first attraction	Second attraction	Third attraction	fourth attraction
First attractor	98.2%	95.1%	90.5%	86.4%
Second attractor	81%	79.4%	64.2%	61.5%
Third attractor	93.5%	89.9%	83.7%	76.4%
fourth attractor	96.7%	91.3%	88.1%	82%

Table 7. Adsorption Kinetic Parameters for Petroleum Hydrocarbon Removal by absorbents.

	1^{st} order kinetics		2^{nd} order kinetics		Intraparticle diffusion		2^{nd} non-Linear Methods	
Absorbent	R^2	$k(min^{-1})$	R^2	$k(min^{-1})$	R^2	$k(min^{-1})$	R^2	$k(min^{-1})$
PPTO	0.93	0.045	0.99	0.098	0.87	0.26	0.97	0.046
GOCB	0.79	0.008	0.98	0.1	0.98	0.33	0.98	0.041
ST	0.92	0.03	0.99	0.11	0.96	0.29	0.95	0.032
CB	0.92	0.033	0.99	0.099	0.95	0.4	0.96	0.037

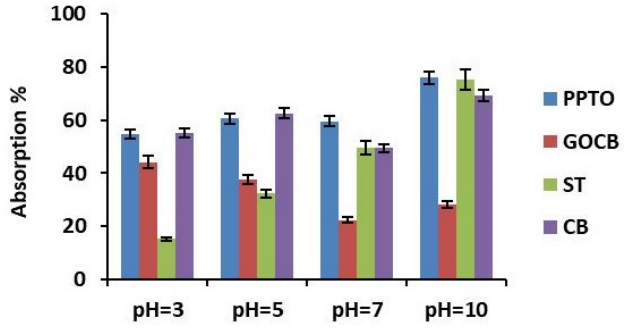

Figure 15. Repeatability of tests.

3.1.7 The repeatability of the performed tests:

The repeatability of the performed tests should be mentioned and error bars should be added in the presented charts. Reproducibility was done three times, and the percentage of error was determined on the graphs. The percentage of error was less than 5% for all Nano absorbents (Tables 6 and 7).

3.1.8 Adsorption kinetic parameters for petroleum hydrocarbon removal by absorbents

4. Conclusion

The study found that the cost of producing and using these adsorbents is very affordable. All 5 adsorbents showed suitable removal levels, and each purification system can be used separately to remove the mentioned absorbers. A combined adsorbent made of straw and polypropylene can effectively remove petroleum hydrocarbons. We tested PPTO, GOCB, straw, and their combination for removing petroleum compounds from water. The combined PPTO nanocomposite removed 97% of petroleum hydrocarbons at a concentration of 10 mg/L. Straw had an absorption rate of 93%, while GOCB had the lowest at 80%. The optimal pH for PPTO, straw, and CB was 10, while GOCB performed best at pH 3. Increasing the adsorbent dosage improved pollutant removal, but concentrations beyond the optimal level did not enhance performance.

PPTO had constant adsorption after 120 minutes, while GOCB showed a continuous increase up to 160 minutes. Combining adsorbents increased adsorption capacity up to 180 minutes. Furthermore, we found that PPTO followed the Temkin isotherm, while GOCB, straw, and the CB groups followed the Langmuir isotherm. Adsorption was spontaneous and exothermic, with higher temperatures improving removal efficiency.

In conclusion, the polypropylene-titanium dioxide nanocomposite and the combination of adsorbents show promise for effectively removing petroleum hydrocarbons from oil-contaminated water. Our analysis outcomes are detailed in Table 4 and were obtained using optimal condition-treated adsorbent. Hexane was used for extraction, and the analysis was conducted using an Agilent GC device. In Iran, the study of the applications of iron oxides Nano-absorbents has been more distributed in research, which may be due to the availability and ease of manufacturing these Nano-absorbents. This is while the distribution of domestic and foreign research on carbon nanotubes has almost the same distribution. Silver nanoparticles have high antibacterial properties and can be used to remove viruses, bacteria and fungi from water and wastewater, but they have been less investigated in domestic research. Although significant progress has been made in the field of using nanoparticles in water and wastewater treatment systems, there are restrictions for nanoparticles in terms of water applications in the form of laws and regulations as well as potential health risks. Therefore, researches on the development of nanoparticles compatible with living organisms have been proposed and with targeted researches in the field of industrial applications of these nanoparticles, it is possible to preserve the environment and restore water resources while promoting and improving the operation of the purification system.

Acknowledgments

We formally acknowledge and express our gratitude to the personnel of the Research Institute of Petroleum Industry in Iran for their invaluable assistance in our research project.

Authors contributions
Authors have contributed equally in preparing and writing the manuscript.

Availability of data and materials
The data that support the findings of this study are available from the corresponding author upon reasonable request.

Conflict of interests
The authors declare that they have no known competing financial interests or personal relationships that could have appeared to influence the work reported in this paper.

References

[1] N. Terbish, S. R. Popuri, and C.-H. C. H. Lee. "Improved performance of organic-inorganic nanocomposite membrane for bioelectricity generation and wastewater treatment in microbial fuel cells.". *Fuel*, 332:126167, 2023.
DOI: https://doi.org/10.1016/j.fuel.2022.126167.

[2] S. R. Barman, P. Banerjee, A. Mukhopadhayay, and P. Das. "Biopolymer linked activated carbon-Nano-bentonite composite membrane for efficient elimination of PAH mixture from aqueous solutions. Biomass Convers.". *Biorefinery*, pages 1–15, 2022.
DOI: https://doi.org/10.1007/s13399-021-02223-0.

[3] R. Gajera, R. V. Patel, A. Yadav, and P. K. Labhasetwar. "Adsorption of cationic and anionic dyes on photocatalytic flyash/TiO2 modified chitosan biopolymer composite.". *J. Water Process Eng.*, 49:102993, 2022.
DOI: https://doi.org/10.1016/j.jwpe.2022.102993.

[4] G. Kour, P. K. Majhi, A. Bharti, R. Kothari, A. Jain, A. Singh, V. V. Tyagi, and D. Pathania. "Biopolymer-Based Nanocomposites and Water Treatment: A Global Outlook. In Biorenewable Nanocomposite Materials, Vol. 2: Desalination and Wastewater Remediation; ACS Symposium Series.". *American Chemical Society: Washington, DC, USA*, 1411:2–25, 2022.
DOI: https://doi.org/10.1021/bk-2022-1411.ch002.

[5] A. I. Osman, E. M. A. El-Monaem, A. M. Elgarahy, C. O. Aniagor, M. Hosny, M. Farghali, E. Rashad, M. I. Ejimofor, E. A. López-Maldonado, and I. Ihara. "Methods to prepare biosorbents and magnetic sorbents for water treatment: A review. ". *Environ. Chem. Lett.*, 21:2337–2398, 2023. URL https://link.springer.com/article/10.1007/s10311-023-01603-4.

[6] J. F. Nure and T. T. I. Nkambule. "The recent advances in adsorption and membrane separation and their hybrid technologies for micropollutants removal from wastewater.". *J. Ind. Eng. Chem.*, 126:92–114, 2023.
DOI: https://doi.org/10.1016/j.jiec.2023.06.034.

[7] A. H. Mostafavi, A. K. Mishra, F. Gallucci, J. H. Kim, M. Ulbricht, A. M. Coclite, and S. S. Hosseini. "Advances in surface modification and functionalization for tailoring the characteristics of thin films and membranes via chemical vapor deposition techniques.". *J. Appl. Polym.*, Sci.140(e53720), 2023.
DOI: https://doi.org/10.1002/app.53720.

[8] I. Suyambulingam, L. Gangadhar, S. S. Sana, D. Divakaran, S. Siengchin, L. A. Kurup, J. Iyyadurai, and K. E. Albert Bernad Noble. "Chitosan Biopolymer and Its Nanocomposites: Emerging Material as Adsorbent in Wastewater Treatment.". *Adv. Mater. Sci. Eng.*, 9387016, 2023.
DOI: https://doi.org/10.1155/2023/9387016.

[9] R. Jiang, T. T. Shen, H. Y. Zhu, Y. Q. Fu, S. T. Jiang, J. B. Li, and J. L. Wang. "Magnetic Fe3O4 embedded chitosan–crosslinked-polyacrylamide composites with enhanced removal of food dye: Characterization, adsorption and mechanism.". *Int. J. Biol. Macromol.*, 227:1234–1244, 2023.
DOI: https://doi.org/10.1016/j.ijbiomac.2022.11.310.

[10] N. Pirestani, M. H. Abolhasani, and F. S. Amin javaheri. "Investigating the Use of Straw in Removing Oil Pollution from Water.". *J Environment and Water Engineering*, 4(1):12–22, 2018.
DOI: https://doi.org/10.22038/jreh.2019.37649.1270.

[11] J. Wang, J. Zhang, L. Han, J. Wang, L. Zhu, and H. Zeng. "Graphene-based materials for adsorptive removal of pollutants from water and underlying interaction mechanism.". *Advances in Colloid and Interface Science*, 289:102360, 2021.
DOI: https://doi.org/10.1016/j.cis.2021.102360.

[12] N. Politaeva, A. Yakovlev, E. Yakovleva, V. Chelysheva, K. Tarantseva, S. Efremova, and S. Ilyashenko. "Graphene Oxide-Chitosan Composites for Water Treatment from Copper Water.". 2022.
DOI: https://doi.org/10.3390/w14091430.

[13] Y. Qi, M. Yang, W. Xu, S. He, and Y. Men. "Natural polysaccharides-modified graphene oxide for adsorption of organic dyes from aqueous solutions.". 2021.
DOI: https://doi.org/10.1016/j.jcis.2016.09.058.

[14] M. Ghorbani, M. Hassan Vakili, and E. Ameri. "Fabrication and evaluation of a biopolymer-based nanocomposite membrane for oily wastewater treatment.". *Mater. Today Commun.*, 28:102560.
DOI: https://doi.org/10.1016/j.mtcomm.2021.102560.

[15] Sadeghi. "The use of nanotechnology in the transfer of probiotics". 2023. URL https://civilica.com/doc/1824944.

[16] S. O. Akpotu, P. N. Diagboya, I. A. Lawal, S. O. Sanni, A. Pholosi, M. G. Peleyeju, F. M. Mthunzi, and A. E. Oromia. "Designer composite of montmorillonite-reduced graphene oxide-PEG polymer for water treatment: Enrofloxacin sequestration and cost analysis.". *Chem. Eng. J.*, 453:139771, 2023.
DOI: https://doi.org/10.1016/j.cej.2022.139771.

[17] M. Schelling, K. Patil, and T. B. Boving. "Sustainable Water Treatment with Induced Bank Filtration.". *Water*, 15:361, 2023.
DOI: https://doi.org/10.3390/w15020361.

[18] I. C. Ossai, A. Ahmed, A. Hassan, and F. S. J. E. T. Hamid. "Innovation. Remediation of soil and water contaminated with petroleum hydrocarbon: A review.". 17:100526, 2020.
DOI: https://doi.org/10.1016/j.eti.2019.100526.

[19] Y. Xiao, L. Chen, Q. Li, X. Zhang, Z. Bai, and K. J. J. S. E. Wang. "Identification and determination of the thermophysical properties of coal at lower temperature.". 18:137–41, 2018.
DOI: https://doi.org/10.1016/S0045-6535(03)00710-0.

[20] O. O. Alegbeleye, B. O. Opeolu, and V. A. J. E. M. Jackson. "Polycyclic aromatic hydrocarbons: a critical review of environmental occurrence and bioremediation.". 60:758–83, 2017.
DOI: https://doi.org/10.1371/journal.pone.0041305.

[21] L. Mohammadi, A. Rahdar, E. Bazrafshan, H. Dahmardeh, M. A. B. H. Susan, and G. Z. J. P. Kyzas. "Petroleum hydrocarbon removal from wastewaters: a review.". 8(4):447, 2020.
DOI: https://doi.org/10.3390/pr8040447.

[22] N. Walaszczyk and R. J. I. I. O. S. Jasiński. "Removal of petroleum derivative pollutants from the environment: techniques and methods.". 21(4):347–59, 2018.
DOI: https://doi.org/10.17512/ios.2018.4.3.

[23] S. Hashemi. "Reference module in materials science and materials engineering: Elsevier BV.". 2015. URL https://search.worldcat.org/title/reference-module-in-materials-science-and-materials-engineering/oclc/931706797.

[24] B. S. Kaith, R. Jindal, H. Mittal, and K. J. J. O. A. P. S. Kumar. "Synthesis, characterization, and swelling behavior evaluation of hydrogels based on gum ghatti and acrylamide for selective absorption of saline from different petroleum fraction–saline emulsions.". 124 (3):2037–47, 2012.
DOI: https://doi.org/10.1002/app.35238.

[25] L. Naumova, T. Minakova, N. Gorlenko, I. Kurzina, and I. Vasenina. "Oxidative Destruction of Organic Pollutants on the Polypropylene Fiber Modified by Nanodispersed Iron.". 5(7):82, 2018. DOI: https://doi.org/10.3390/environments5070082.

[26] U. Naeem, M. A. J. E. S. Qazi, and P. Research. "Leading edges in bioremediation technologies for removal of petroleum hydrocarbons.". 27(22):27370–82, 2020. DOI: https://doi.org/10.1007/s11356-019-06124-8.

[27] N. Baboli bafkara. "Investigation of Nitrate Removal from Aqueous Solutions by Nano Adsorbent of Wheat Straw.". *Journal of Natural Environment*, 74(3):572–87, 2021. DOI: https://doi.org/10.22059/jne.2021.325138.2229.

[28] C. Liu, Z. Yin, D. Hu, F. Mo, R. Chu, and L. Zhu. "Biochar derived from chicken manure as a green adsorbent for naphthalene removal.". 28:36585–97, 2021. DOI: https://doi.org/10.1007/s11356-021-13286-x.

[29] A. Haruna, F. K. Chong, Y. C. Ho, Z. M. A. J. E. S. Merican, and P. Research. "Preparation and modification methods of defective titanium dioxide-based nanoparticles for photocatalytic wastewater treatment—a comprehensive review.". 29(47):70706–45, 2022. DOI: https://doi.org/10.1007/s11356-022-22749-8.

[30] M. A. Tony. "Low-cost adsorbents for environmental pollution control: a concise systematic review from the prospective of principles, mechanism and their applications.". *Journal of Dispersion Science and Technology*, 43(11):1612–33, 2022. DOI: https://doi.org/10.3390/math11102248.

[31] Kh. Pourshamsian. "Determination of physical, chemical and bacteriological parameters of Gorgan city drinking water.". 2019. URL https://sid.ir/search/journal/paper.

[32] Kh. Pourshamsian. "Qualitative zoning of Talar river using OWQI index and GIS system.". 2020. URL https://civilica.com/doc/201365.

[33] Kh. Pourshamsian. "Investigating the effect and detection of bacterial cells by titanium-coated silver nanoparticles.". 2018. URL https://civilica.com/doc/103746.

[34] R. Szabová, L. Černáková, M. Wolfová, and M. J. A. C. S. Černák. "Coating of TiO_2 nanoparticles on the plasma activated polypropylene fibers.". 2(1):70–6, 2009. DOI: https://doi.org/https://acs.fchpt.stuba.sk/papers/acs-0037.pdf.

[35] Z. Z. Abidin. "Ecofriendly Approach to Adsorption of Congo Red from Aqueous Media Using Chaff Powder from Jatropha curcas Seed (Isotherm and Kinetic Model).". 2019. DOI: https://doi.org/10.5004/dwt.2020.25169.

[36] Szabova. "Heavy metals and their bioavailability from soils in the long-term polluted Central Spiš region of SR.". 2009. DOI: https://doi.org/10.17221/21/2009-PSE.

[37] C. A. Franco, F. B. Cortés, N. N. J. J. O. C. Nassar, and I. science. "Adsorptive removal of oil spill from oil-in-fresh water emulsions by hydrophobic alumina nanoparticles functionalized with petroleum vacuum residue.". 425:168–77, 2014. DOI: https://doi.org/10.1016/j.jcis.2014.03.051.

[38] H. Amani, H. Arzaghi, M. Bayandori, A. S. Dezfuli, H. Pazoki-Toroudi, and A. Shafiee. "Controlling cell behavior through the design of biomaterial surfaces: a focus on surface modification techniques.". 6(13):1900572, 2019. DOI: https://doi.org/10.1002/smll.201000233.

[39] Rahmani. "Effect of nanostructure alumina on adsorption of heavy metals.". 2010. DOI: https://doi.org/10.1016/j.desal.2009.11.027.

[40] Naumova. "A pathway for mitotic chromosome formation. ". 2018. DOI: https://doi.org/10.1126/science.aao6135.

[41] A. Mehmood, F. S. A. Khan, N. M. Mubarak, S. A. Mazari, A. S. Jatoi, and M. Khalid. "Carbon and polymer-based magnetic nanocomposites for oil-spill remediation—a comprehensive review.". 28(39): 54477–96, 2021. DOI: https://doi.org/10.1007/s11356-021-16045-0.

[42] G. H. Sonawane, S. P. Patil, and S. H. Sonawane. "Nanocomposites and its applications.". *Applications of nanomaterials: Elsevier*, pages 1–22, 2018. URL https://link.springer.com/article/10.1007/s42114-023-00808-z.

[43] A. Bendaoued, M. Messaoud, O. Harzallah, S. Bistac, and R. J. J. O. M. R. Salhi. "Technology. Nano-TiO_2 effect on thermal, rheological and structural properties of thermoplastic polypropylene nanocomposites". 17:2313–25, 2022. DOI: https://doi.org/10.1016/j.jmrt.2022.01.114.

[44] L. A. Mokif, H. K. Jasim, and N. A. J. M. T. P. Abdulhusain. "Petroleum and oily wastewater treatment methods: a mini review.". 49:2671–4, 2022. DOI: https://doi.org/10.5772/intechopen.109853.

[45] J. Wang and S. J. C. R. I. E. S. Zhuang. "Removal of various pollutants from water and wastewater by modified chitosan adsorbents.". *Technology*, 47(23):2331–86, 2017. DOI: https://doi.org/10.1080/10643389.2017.1421845.

[46] T. Russo, P. Fucile, R. Giacometti, and F. J. P. Sannino. "Sustainable removal of contaminants by biopolymers: a novel approach for wastewater treatment.". *Current state and future perspectives*, 9(4): 719, 2021. DOI: https://doi.org/10.3390/pr9040719.

[47] A. Ahmad, S. Sumathi, and B. J. W. R. Hameed. "Adsorption of residue oil from palm oil mill effluent using powder and flake chitosan: equilibrium and kinetic studies.". 39(12):2483–94, 2005. DOI: https://doi.org/10.1016/j.watres.2005.03.035.

[48] M. Zaredost and M. Rasoli. "Compare the performance of three kinds of synthetic sorbent for the removal of oil pollution of the sea.". *Fourth National Conference on Safety Engineering and HSE Engineering*, 2011. URL https://ijogst.put.ac.ir/article-4792-25ab8aab3e25e512100d4863b70639f9.pdf.

[49] A. S. Roy, R. Yenn, A. K. Singh, H. P. D. Boruah, N. Saikia, and M. J. A. J. O. B. Deka. "Bioremediation of crude oil contaminated tea plantation soil using two Pseudomonas aeruginosa strains AS 03 and NA 108.". 12(19), 2013. URL https://www.ajol.info/index.php/ajb/article/view/130116.

[50] A. Jadid, S. Shahsavari, A. Seifkordi, and A. V. J. D. O. H. Yazdi. "Adsorption of Phenol in Wastewater Using Nano Grapheme Oxide-Chitosan-Bentonite Absorbent.". 11(4):368–80, 2021. DOI: https://doi.org/10.34172/doh.2020.44.

[51] H. Anjum, K. Johari, A. Appusamy, N. Gnanasundaram, and M. J. J. O. H. M. Thanabalan. "Surface modification and characterization of carbonaceous adsorbents for the efficient removal of oil pollutants.". 379:120673, 2019. DOI: https://doi.org/10.1016/j.jhazmat.2019.05.066.

[52] M. Othman, S. S. Hussin, A. Rambli, and Z. Zahid. "Equilibrium Isotherm Models for the Adsorption of Methylene Blue from Wastewater.". *Journal of Physics: Conference Series: IOP Publishing*, 2019. DOI: https://doi.org/10.1088/1742-6596/1366/1/012033.

[53] D. Schwantes, J. Casarin, A. Pinheiro, I. G. Pinheiro, and G. F. J. A. J. O. A. R. Coelho. "Removal of Cr (III) from contaminated water using industrial waste of the cassava as natural adsorbents.". 10(46): 4241–51, 2015. DOI: https://doi.org/10.5897/AJAR2015.9835.

[54] I. Makertihartha, Z. Rizki, M. Zunita, and P. Dharmawijaya. "Dyes removal from textile wastewater using graphene based nanofiltration.". *AIP Conference Proceedings: AIP Publishing*, 2017. DOI: https://doi.org/10.3390/membranes11040269.

[55] K. Thakur and B. Kandasubramanian. "Graphene and Graphene Oxide-Based Composites for Removal of Organic Pollutants: A Review.". *Journal of Chemical & Engineering Data*, 64(3):833–67, 2019. DOI: https://doi.org/10.1021/acs.jced.8b01057.